

Pervasive duplication of tumor suppressor genes preceded parallel evolution of large bodied Paenungulates

Juan Manuel Vazquez ¹ *, Vincent J Lynch

1 Department of Human Genetics, 920 East 58th St, Chicago, IL, 60637
Department of Biological Sciences, 551 Cooke Hall, Buffalo NY, 14260

* Corresponding author: juanvazquez@uchicago.edu

Abstract

Lorem ipsum dolor sit amet, consectetur adipiscing elit. Curabitur eget porta erat. Morbi consectetur est vel gravida pretium. Suspendisse ut dui eu ante cursus gravida non sed sem. Nullam sapien tellus, commodo id velit id, eleifend volutpat quam. Phasellus mauris velit, dapibus finibus elementum vel, pulvinar non tellus. Nunc pellentesque pretium diam, quis maximus dolor faucibus id. Nunc convallis sodales ante, ut ullamcorper est egestas vitae. Nam sit amet enim ultrices, ultrices elit pulvinar, volutpat risus.

Author summary

Lorem ipsum dolor sit amet, consectetur adipiscing elit. Curabitur eget porta erat. Morbi consectetur est vel gravida pretium. Suspendisse ut dui eu ante cursus gravida non sed sem. Nullam sapien tellus, commodo id velit id, eleifend volutpat quam. Phasellus mauris velit, dapibus finibus elementum vel, pulvinar non tellus. Nunc pellentesque pretium diam, quis maximus dolor faucibus id. Nunc convallis sodales ante, ut ullamcorper est egestas vitae. Nam sit amet enim ultrices, ultrices elit pulvinar, volutpat risus.

Introduction

One of the major constraints on the evolution of large body sizes in animals is an increased risk of developing cancer. If all cells in all organisms have a similar risk of malignant transformation and equivalent cancer suppression mechanisms, organism with many cells should have a higher prevalence of cancer than organisms with fewer cells. Consistent with this expectation there is a strong positive correlation between body size and cancer incidence within species, for example, human cancer incidence increases with increasing adult height [1,2] and cancer incidence is positively correlated with body size in dogs [???,3]. There is no correlation, however, between body size and cancer risk between species. This lack of correlation is often referred to as ‘Peto’s Paradox’ [4–6]. While it is clear that a resolution to Peto’s Paradox must involve the evolution of enhanced cancer protection alongside increases in body size and lifespan, the specific genetic, molecular, and cellular mechanisms that underlie this resistance have proven elusive. [7–11].

Among the challenges for discovering how animals evolved enhanced cancer protection mechanisms is identifying lineages in which large bodied species are nested within species with small body sizes. Afrotherian mammals are generally small-bodied, similarly to the predicted common ancestor of Eutherian mammals. For example, maximum adult weights are ~70g in golden moles, ~120g in tenrecs, ~170g in elephant shrews, ~3kg in hyraxes, and 60kg in armadillos [12]. However, while these extant species are relatively small, the fossil evidence demonstrates that their ancestral lineages reached enormous sizes. For example, while extant hyraxes are relatively small, the extinct Titanohyrax is estimated to have weighed up to ~1300kg [13]. The largest members of Afrotheria, too, are dwarfed by the size of their recent ancestors: extant cows manatees are large bodied (~322-480kg) but are relatively small compared to the extinct Stellar's sea cow which is estimated to have weight 8000-10000kg [14]. Similarly African (4,800kg) and Asian elephants (3,200kg) are the largest living elephant species, but are dwarfed by the truly gigantic extinct Proboscideans such as Deinotherium (~132,000kg), Mammuthus borsoni (110,000kg), and the Asian straight-tusked elephant (~220,000kg), the largest known land mammal [15]. Remarkably these large-bodied Afrotherian lineages are nested within small bodied species (Fig. 1) [16–19], indicating that gigantism independently evolved in hyraxes, sea cows, and elephants (Paenungulates). Thus, Paenungulates are an excellent model system in which to explore the mechanisms that underlie the evolution of large body sizes and augmented cancer resistance.

Although many mechanisms can potentially resolve Peto's paradox, the most parsimonious route to enhanced cancer resistance is likely through an increased copy number of tumor suppressors. Such an example has been seen in the case of candidate genes such as *TP53* and *LIF* [11,20,21] as well as in studies involving a limited set of candidate genes [22,23]. As these studies focus on *a priori* gene sets, however, it remains unknown whether this is a general, genome-wide trend in Afrotherian genomes; and whether such a general trend is associated with the recent increases in body size – and therefore expected cancer risk – in these species.

Here, we trace the evolution of body mass and gene copy number variation in Afrotherians in order to investigate whether gene duplications are enriched in large, long-lived species for genes involved in known tumor suppression pathways. Our estimates of the evolution of body mass, similarly to previous studies [16–19], show that large body masses evolved in a step-wise manner, with major increases in body mass in the Pseudungulata (17kg), Paenungulata (25kg), Tethytheria (296kg), and Proboscidea (4,100kg) stem-lineages. Furthermore, we see that the ancestral body size increases in Hydracoidia and Sirenia were independent events. To study the evolution of gene copy number, we used a genome-wide Reciprocal Best BLAT Hit (RBBH) method to identify gene duplications in Afrotherian genomes, and used parsimony to infer the lineages in which those duplications occurred. We found gene duplications in lineages with increased body mass were enriched in functions related to tumor suppression, including regulation of the cell cycle, DNA damage repair, and regulation of apoptosis. These data suggest that duplication of tumor suppressors played a role in the evolution of large, long-lived in Afrotherians.

Methods

Ancestral Body Size Reconstruction

We built a time-calibrated supertree of Eutherian mammals by combining the time-calibrated molecular phylogeny of Bininda-Emonds *et al.* [24] with the time-calibrated total evidence Afrotherian phylogeny from Puttick and Thomas [???].

While the Bininda-Emonds *et al.* [24] phylogeny includes 1,679 species, only 34 are Afrotherian, and no fossil data are included. The inclusion of fossil data from extinct species is essential to ensure that ancestral state reconstructions of body mass are not biased by only including extant species. This can lead to inaccurate reconstructions, for example, if lineages convergently evolved large body masses from a small bodied ancestor. In contrast, the total evidence Afrotherian phylogeny of Puttick and Thomas [19] includes 77 extant species and fossil data from 39 extinct species. Therefore we replaced the Afrotherian clade in the Bininda-Emonds *et al.* [24] phylogeny with the Afrotherian phylogeny of Puttick and Thomas [19] using Mesquite. Next, we jointly estimated rates of body mass evolution and reconstructed ancestral states using a generalization of the Brownian motion model that relaxes assumptions of neutrality and gradualism by considering increments to evolving characters to be drawn from a heavy-tailed stable distribution (the “Stable Model”) [25]. The stable model allows for occasional large jumps in traits and has previously been shown to out-perform other models of body mass evolution, including standard Brownian motion models, Ornstein–Uhlenbeck models, early burst maximum likelihood models, and heterogeneous multi-rate models [25].

Identification of Duplicate Genes

Reciprocal Best-Hit BLAT: We developed a reciprocal best hit BLAT (RBHB) pipeline to quickly identify homologs and estimate gene copy numbers (**Figure 1A**). The Reciprocal Best Hit (RBH) search strategy is conceptually straightforward: 1) Given a gene of interest GA in a query genome A, one searches a target genome B for all possible matches to GA; 2) For each of these hits, one then performs the reciprocal search in the original query genome to identify the highest-scoring hit; 3) A hit in genome B is defined as a homolog of gene GA if and only if the original gene GA is the top reciprocal search hit in genome A. We selected BLAT [26] as our algorithm of choice, as this algorithm is sensitive to highly similar (>90% identity) sequences, thus identifying the highest-confidence homologs while minimizing many-to-one mapping problems when searching for multiple genes. RBH performs similar to other more complex methods of orthology prediction, and is particularly good at identifying incomplete genes that may be fragmented in low quality/poor assembled regions of the genome [???,27].

Effective Copy Number By Coverage: In lower-quality genomes, many genes are fragmented across multiple scaffolds, which results in BLAT calling multiple hits when in reality there is only one gene. To compensate for this, we came up with a novel statistic, Estimated Copy Number by Coverage (ECNC), which averages the number of times we see each nucleotides of a query sequence in a target genome over the total number of nucleotides of the query sequence found overall in each target genome (**Figure 1B**; Supplementary Figure 1). This allows us to correct for genes that have been fragmented across incomplete genomes, without underestimating the copy number of proteins that lack domains found in the human sequence.

RecSearch Pipeline: We created a custom Python pipeline for automating RBHB searches between a single reference genome and multiple target genomes using a list of query sequences from the reference genome. For the query sequences in our search, we used the hg38 Proteome provided by UniProt [28], which is a comprehensive set of protein sequences curated from a combination of predicted and validated protein sequences generated by the UniProt Consortium. In order to refine our search, we omitted protein sequences originating from long, noncoding RNA loci (e.g. LINC genes); poorly-studied genes from predicted open reading frames (C-ORFs); and sequences with highly repetitive sequences such as zinc fingers, protocadherins, and transposon-containing genes, as these were prone to high levels of false positive hits. After filtering out problematic protein queries, we then used our pipeline (Figure 1A) to

search for all copies of our 20456 query genes in publicly available Afrotherian genomes, including African savannah elephant (*Loxodonta africana*: loxAfr3, loxAfr4, loxAfrC), African forest elephant (*Loxodonta cyclotis*: loxCycF), Asian Elephant (*Elephas maximus*: eleMaxD), Woolly Mammoth (*Mammuthus primigenius*: mamPriV), Colombian mammoth (*Mammuthus columbi*: mamColU), American mastodon (*Mammut americanum*: mamAmelI), Rock Hyrax (*Procapia capensis*: proCap1, proCap2, proCap2.HiC), West Indian Manatee (*Trichechus manatus latirostris*: triManLat1, triManLat1.HiC), Aardvark (*Orycteropus afer*: oryAfe1, oryAfe1.HiC), Lesser Hedgehog Tenrec (*Echinops telfairi*: echTel2), Nine-banded armadillo (*Dasypus novemcinctus*: dasNov3), Hoffman’s two-toed sloth (*Choloepus hoffmannii*: choHof1, choHof2, choHof2.HiC), Cape golden mole (*Chrysochloris asiatica*: chrAsi1), and Cape elephant shrew (*Elephantulus edwardii*: eleEdw1). For many of these species, we covered multiple assemblies in order to test the effects of assembly size and quality on our hits.

Duplication gene inclusion criteria: In order to condense transcript-level hits into single gene loci, and to resolve many-to-one genome mappings, we removed exons where transcripts from different genes overlapped, and merged overlapping transcripts of the same gene into a single gene locus call. The resulting gene-level copy number table was then combined with the maximum ECNC values observed for each gene in order to call gene duplications. We called a gene duplicated if its copy number was two or more, and if the maximum ECNC value of all the gene transcripts searched was 1.5 or greater; previous studies have shown that incomplete duplications can encode functional genes, therefore partial gene duplications were included provided they passed additional inclusion criteria. The ECNC cut off of 1.5 was selected empirically, as this value minimized the number of false positives seen in a test set of genes and genomes. The results of our initial search are summarized in Figure 1B. Overall, we identified [MEDIAN] genes across all species, or [%HITS/QUERIES] of our starting query genes. As expected, there was a correlation between the number of hits identified in a species with the evolutionary distance relative to humans [Sup Figure 1].

Duplicate gene exclusion criteria: We excluded genes from downstream analyses for which assignment of homology was uncertain, including uncharacterized ORFs (17), LOC (17), HLA genes (17), replication dependent histones (17), odorant receptors (17), ribosomal proteins (17), zinc finger transcription factors (17), viral and repetitive-element-associated proteins (17) and any protein described as either “Uncharacterized,” “Putative,” or “Fragment” by UniProt in UP000005640 (17).

Evidence for Functionality of Identified Genes

To validate and filter out RBHB results, we intersected our results with either gene prediction or transcriptomic evidence as a proxy for functionality.

Transcriptome Assembly: For the African Savana Elephant, Asian Elephant, West Indian Manatee, and Nine-Banded Armadillo, we generated *de novo* transcriptomes using publically-available RNA-sequencing data from NCBI SRA. We mapped reads to all genomes available for each species, and assembled transcripts using HISAT2 and StringTie, respectively [???,??,??]. RNA-sequencing data was not available for Cape Golden Mole, Cape Elephant Shrew, Rock Hyrax, Aardvark, or the Lesser Hedgehog Tenrec.

Gene Prediction: We obtained tracks for genes predicted using GenScan for all the genomes available via UCSC Genome Browser: African savannah elephant (loxAfr3), Rock Hyrax (proCap1), West Indian Manatee (triManLat1), Aardvark (oryAfe1), Lesser Hedgehog Tenrec (echTel2), Nine-banded armadillo (dasNov3), Hoffman’s Two-Toed Sloth (choHof1), Cape golden mole (chrAsi1), and Cape Elephant Shrew (eleEdw1); gene prediction tracks for higher-quality assemblies were not available.

Evidenced Duplicate Criteria: We intersected our records of duplicate hits identified in each genome with the gene prediction tracks and/or transcriptome assemblies using `bedtools` [???]. When multiple lines of evidence for functionality were present for a genome, we used the union of all intersections as the final output for evidenced duplicates. When analyzing the highest-quality assemblies available for each species, if a species had neither gene prediction tracks nor RNA-seq data for the highest-quality genome available, we conservatively included all hits for the genome in the final set of evidenced duplicates.

Reconstruction of Ancestral Copy Numbers

We implemented a maximum likelihood method for determining the ancestral copy numbers of genes in *Atlantogenata* using IQ-Tree. For this analysis, we used an unrooted subset of our prior species tree, including only the aforementioned *Atlantogenata* species. We generated PHYLIP files containing the copy number of each gene in the highest quality genome for each species, encoding genes on a scale from 1-31+ copies as 1-9, A-V; and encoding a gene's copy number as uncertain ("?) when we did not identify it in the genome. We used the included tree-searching and model-testing functionality in IQ-Tree to determine the most likely topology for the species tree, and to obtain the most likely model for copy number changes in the genome. We defined the ancestral state of a node if it had greater than an 80% posterior probability.

Pathway Enrichment Analysis

To determine which pathways were associated with duplicated genes in each species and lineage, we used WEBGESTALT to perform overrepresentation analysis (ORA) of the duplicated gene lists relative to our initial query gene list. For the database of pathways used in the analysis, we used Reactome [???], Wikipathways and Wikipathways.cancer [???], and KEGG [???].

Results

```
## Warning: Tried to calculate with group_by(), but the calculation failed.
## Falling back to ungrouped filter operation...

## Warning: Tried to calculate with group_by(), but the calculation failed.
## Falling back to ungrouped filter operation...

## Warning in geom2trace.default(dots[[1L]][[3L]], dots[[2L]][[1L]], dots[[3L]]
##   If you'd like to see this geom implemented,
##   Please open an issue with your example code at
##   https://github.com/ropensci/plotly/issues

## Warning in geom2trace.default(dots[[1L]][[3L]], dots[[2L]][[1L]], dots[[3L]]
##   If you'd like to see this geom implemented,
##   Please open an issue with your example code at
##   https://github.com/ropensci/plotly/issues

## Warning in geom2trace.default(dots[[1L]][[3L]], dots[[2L]][[1L]], dots[[3L]]
##   If you'd like to see this geom implemented,
##   Please open an issue with your example code at
##   https://github.com/ropensci/plotly/issues
```

Step-wise evolution of large, long-lived Afrotherians

211

Warning: Removed 120 rows containing missing values (geom_image).

212

Table 1. A table generated by the longtable package.

Ancestor/Species	Estimated Body Size (log(g))	95% CI (Low)	95% CI (High)
Cryptochloris wintoni	3.13	3.13	3.13
Amblysomus marleyi	3.53	3.53	3.53
Elephantulus revoili	3.48	3.48	3.48
Titanohyrax andrewsi	12.97	12.97	12.97
Titanohyrax ultimus	14.08	14.08	14.08
Megalohyrax sp nov	12.52	12.52	12.52
Elephas maximus asurus	15.66	15.66	15.66
Protenrec tricuspis	1.14	1.14	1.14
Microgale parvula	1.16	1.16	1.16
Microgale pusilla	1.25	1.25	1.25
Geogale aurita	1.90	1.90	1.90
Microgale longicaudata	2.09	2.09	2.09
Microgale brevicaudata	2.19	2.19	2.19
Microgale jobihely	2.30	2.30	2.30
Microgale principula	2.32	2.32	2.32
Dilambdogale gheerbranti	2.38	2.38	2.38
Microgale taiva	2.47	2.47	2.47
Microgale cowani	2.62	2.62	2.62
Eremitalpa granti	3.14	3.14	3.14
Calcochloris obtusirostris	3.27	3.27	3.27
Neamblysomus julianae	3.33	3.33	3.33
Chlorotalpa duthieae	3.38	3.38	3.38
Chlorotalpa sclateri	3.54	3.54	3.54
Macroscelides proboscideus	3.64	3.64	3.64
Chrysochloris stuhlmanni	3.74	3.74	3.74
Oryzorictes hova	3.79	3.79	3.79
Elephantulus myurus	3.81	3.81	3.81
Elephantulus brachyrhynchus	3.81	3.81	3.81
Elephantulus rozeti	3.81	3.81	3.81
Elephantulus fuscus	3.82	3.82	3.82
Elephantulus intufi	3.82	3.82	3.82
Microgale talazaci	3.88	3.88	3.88
Chrysochloris asiatica	3.89	3.89	3.89
Elephantulus edwardii	3.90	3.90	3.90
Carpitalpa arendsi	3.94	3.94	3.94
Amblysomus corriae	3.94	3.94	3.94
Amblysomus hottentotus	3.98	3.98	3.98
Elephantulus fuscipes	4.04	4.04	4.04
Elephantulus rufescens	4.05	4.05	4.05
Neamblysomus gunningi	4.09	4.09	4.09
Elephantulus rupestris	4.12	4.12	4.12
Amblysomus septentrionalis	4.23	4.23	4.23
Chambius kasserinensis	4.27	4.27	4.27
Amblysomus robustus	4.33	4.33	4.33
Micropotamogale lamottei	4.36	4.36	4.36
Echinops telfairi	4.47	4.47	4.47

Ancestor/Species	Estimated Body Size (log(g))	95% CI (Low)	95% CI (High)
Limnogale mergulus	4.52	4.52	4.52
Hemicentetes semispinosus	4.75	4.75	4.75
Chrysospalax villosus	4.77	4.77	4.77
Petrodromus tetradactylus	5.29	5.29	5.29
Herodotius pattersoni	5.50	5.50	5.50
Setifer setosus	5.61	5.61	5.61
Rhynchocyon cirnei	5.86	5.86	5.86
Metoldobotes sp nov	5.93	5.93	5.93
Chrysospalax trevelyani	6.13	6.13	6.13
Rhynchocyon petersi	6.15	6.15	6.15
Rhynchocyon chrysopygus	6.28	6.28	6.28
Potamogale velox	6.49	6.49	6.49
Rhynchocyon udzungwensis	6.57	6.57	6.57
Tenrec ecaudatus	6.75	6.75	6.75
Dasypus sabanicola	7.05	7.05	7.05
Tolypeutes matacus	7.11	7.11	7.11
Dasypus septemcinctus	7.30	7.30	7.30
Zaedyus pichiy	7.31	7.31	7.31
Dasypus hybridus	7.31	7.31	7.31
Chaetophractus villosus	7.61	7.61	7.61
Chaetophractus nationi	7.67	7.67	7.67
Heterohyrax brucei	7.78	7.78	7.78
Cabassous centralis	7.92	7.92	7.92
Seggeurius amourensis	7.98	7.98	7.98
Procavia capensis	8.01	8.01	8.01
Dendrohyrax dorsalis	8.06	8.06	8.06
Microhyrax lavocati	8.13	8.13	8.13
Bradypus tridactylus	8.23	8.23	8.23
Bradypus torquatus	8.27	8.27	8.27
Dasypus novemcinctus	8.37	8.37	8.37
Euphractus sexcinctus	8.43	8.43	8.43
Choloepus hoffmanni	8.47	8.47	8.47
Bradypus variegatus	8.49	8.49	8.49
Tamandua tetradactyla	8.52	8.52	8.52
Cyclopes didactylus	8.53	8.53	8.53
Choloepus didactylus	8.71	8.71	8.71
Thyrohyrax meyeri	8.78	8.78	8.78
Saghatherium boweni	9.13	9.13	9.13
Dasypus kappleri	9.23	9.23	9.23
Thyrohyrax domorictus	9.30	9.30	9.30
Dimaitherium patnaiki	9.57	9.57	9.57
Phosphatherium escuilliei	9.62	9.62	9.62
Saghatherium antiquum	9.73	9.73	9.73
Thyrohyrax litholagus	10.01	10.01	10.01
Myrmecophaga tridactyla	10.26	10.26	10.26
Myorycteropus africanus	10.27	10.27	10.27
Selenohyrax chatrathi	10.73	10.73	10.73
Priodontes maximus	10.82	10.82	10.82
Orycteropus afer	10.87	10.87	10.87
Antilohyrax pectidens	10.93	10.93	10.93
Bunohyrax fajumensis	11.32	11.32	11.32

Ancestor/Species	Estimated Body Size (log(g))	95% CI (Low)	95% CI (High)
Afrohyrax championi	11.32	11.32	11.32
Geniohyus mirus	11.33	11.33	11.33
Prorastomus sirenoides	11.49	11.49	11.49
Elephas antiquus falconeri	11.51	11.51	11.51
Pachyhyrax crassidentatus	11.81	11.81	11.81
Megalohyrax eocaenus	11.95	11.95	11.95
Elephas cypriotes	12.21	12.21	12.21
Bunohyrax major	12.36	12.36	12.36
Titanohyrax angustidens	12.48	12.48	12.48
Daouitherium rebouli	12.80	12.80	12.80
Arcanotherium savagei	12.89	12.89	12.89
Dugong dugon	12.92	12.92	12.92
Trichechus senegalensis	13.03	13.03	13.03
Trichechus inunguis	13.08	13.08	13.08
Protosiren smithae	13.20	13.20	13.20
Numidotherium koholense	13.23	13.23	13.23
Omanitherium dhofarensis	13.35	13.35	13.35
Trichechus manatus	13.44	13.44	13.44
Moeritherium spp	13.82	13.82	13.82
Phiomia spp	13.89	13.89	13.89
Elephas maximus	15.02	15.02	15.02
Barytherium spp	15.20	15.20	15.20
Mammuthus primigenius	15.27	15.27	15.27
Mammut borsoni	16.49	16.49	16.49
Mammuthus trogontherii	16.38	16.38	16.38
Loxodonta africana	15.35	15.35	15.35
Loxodonta cyclotis	15.37	15.37	15.37
Palaeoloxodon antiquus	16.14	16.14	16.14
Palaeoloxodon namadicus	16.81	16.81	16.81
Mammut americanum	15.61	15.61	15.61
Mammuthus columbi	15.71	15.71	15.71
Hydrodamalis gigas	15.72	15.72	15.72
Atlantogenata	5.55	4.06	7.99
Afrotheria	5.55	4.05	7.99
Afrosorcida	4.35	2.58	6.13
Macroscelidae	5.27	3.98	6.81
Pseudoungulata	9.76	5.21	12.71
Paenungulata	10.13	7.24	13.02
Tethytheria	12.60	10.25	13.81
Proboscidae	15.23	14.22	16.24
Elephantidae	15.49	14.89	16.10
Elephantina	15.51	15.08	15.99
Mammuthus	15.54	15.24	15.84
Loxodontini	15.55	15.02	16.10
Loxodonta	15.72	15.16	16.30
Xenarthra	7.57	5.96	9.18

To trace the evolutionary history of body mass and lifespan in Afrotherians, we built a time-calibrated supertree of Eutherian mammals combining 1,679 species from Bininda-Emonds et al [24] with a total evidence Afrotherian phylogeny including 77 extant and fossil data from 39 extinct species [19]. Fossil data from extinct species were

included to ensure that ancestral state reconstructions of body mass in Afrotherians were not biased by only including extant species, which can lead to inaccurate reconstructions, for example, if lineages multiple lineages evolved large body masses from a small bodied ancestor. We jointly estimated rates of body mass evolution and reconstructed ancestral states using a generalization of a Brownian model of character evolution, which allows for occasional large jumps in traits (stable model) and out performs standard Brownian motion and Ornstein-Uhlenbeck models of character evolution [25].

Similar to previous studies of Afrotherian body size [19,25], we found that the body mass of the Afrotherian ancestor was inferred to be small (0.26kg, 95% CI: 0.31-3.01kg) and that substantial accelerations in the rate of body mass evolution occurred coincident with a 65× increase in body mass in the stem-lineage of *Pseudungulata* (17kg), a 1.5× increase in body mass in the stem-lineage of *Paenungulata* (25kg), a 12× increase in body mass in the stem-lineage of *Tethytheria* (296kg), and a 14× increase in body mass in the stem-lineage of *Proboscidea* (4,100kg; Figure 1). The ancestral *Hyracoidea* was inferred to be relatively small (2.86-15.71kg), and rate accelerations were coincident with independent body mass increases in large hyraxes such as *Titanohyrax andrewsi* (67× increase in body mass). While the body mass of the ancestral *Sirenian* was inferred to be large (61-656kg), a rate acceleration occurred coincident with a 10× body mass increase in Stellar’s sea cow. Rate accelerations also occurred coincident with 36× body mass reduction in the stem-lineage of the dwarf elephants *Elephas (Palaeoloxodon) falconeri* and *Palaeoloxodon cypriotes*. These data suggest that gigantism in *Afrotherians* evolved step-wise, from small to medium bodies in the *Pseudungulata* stem-lineage, medium to large bodies in the *Tethytherian* stem-lineage and extinct hyraxes, and from large to exceptionally large bodies independently in the *Proboscidean* stem-lineage and Stellar’s sea cow (Figure 1).

Pervasive duplication of tumor suppressors during the origins of large bodied Afrotheirans

Warning: Column ‘Genome’ joining factor and character vector, coercing into character vector

Warning in melt(., na.rm = T): The melt generic in data.table has been passed a matrix and will attempt to redirect to the relevant reshape2 method; please note that reshape2 is deprecated, and this redirection is now deprecated as well. ## To continue using melt methods from reshape2 while both libraries are attached e.g. melt.list, you can prepend the namespace like reshape2::melt(.). In the next version, this warning will become an error.

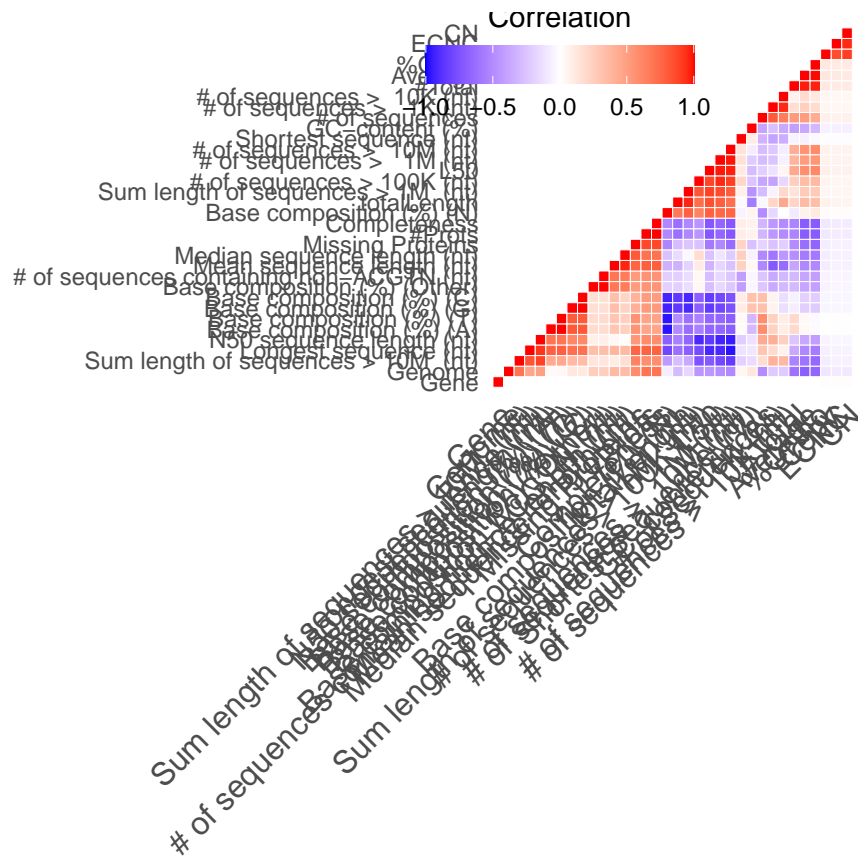
	Var1	Var2	value
## 1	Gene	Copy	0.011177676
## 2	Genome	Copy	-0.104365173
## 3	Sum length of sequences > 10M	(nt) Copy	-0.074960529
## 4	Longest sequence	(nt) Copy	-0.067231077
## 5	N50 sequence length	(nt) Copy	-0.050741921
## 6	Base composition (%)	(A) Copy	-0.001502967
## 7	Base composition (%)	(T) Copy	-0.001379093
## 8	Base composition (%)	(G) Copy	-0.043271156
## 9	Base composition (%)	(C) Copy	-0.042268177
## 10	Base composition (%)	(Other) Copy	-0.050228064
## 11	# of sequences containing non-ACGTN	(nt) Copy	-0.050621596
## 12	Mean sequence length	(nt) Copy	-0.074983744

## 13	Median sequence length (nt)	Copy	-0.074897040	266
## 14	Missing Proteins	Copy	-0.079692396	267
## 15	#Prots	Copy	-0.101300994	268
## 16	Completeness	Copy	-0.101321644	269
## 17	Base composition (%) (N)	Copy	0.019768158	270
## 18	totalLength	Copy	0.067454870	271
## 19	Sum length of sequences > 1M (nt)	Copy	0.051354838	272
## 20	# of sequences > 100K (nt)	Copy	0.056049593	273
## 21	L50	Copy	0.082175611	274
## 22	# of sequences > 1M (nt)	Copy	0.074461957	275
## 23	# of sequences > 10M (nt)	Copy	0.075679451	276
## 24	Shortest sequence (nt)	Copy	-0.013216232	277
## 25	GC-content (%)	Copy	-0.064591581	278
## 26	# of sequences	Copy	0.076630197	279
## 27	# of sequences > 1K (nt)	Copy	0.047474518	280
## 28	# of sequences > 10K (nt)	Copy	0.045583001	281
## 29	#Total	Copy	0.116391876	282
## 30	Average	Copy	0.124341009	283
## 31	%Ortho	Copy	0.120616153	284
## 32	Gene	ECNC	0.011137324	285
## 33	Genome	ECNC	-0.090522003	286
## 34	Sum length of sequences > 10M (nt)	ECNC	-0.061380983	287
## 35	Longest sequence (nt)	ECNC	-0.053145168	288
## 36	N50 sequence length (nt)	ECNC	-0.040007282	289
## 37	Base composition (%) (A)	ECNC	0.004626621	290
## 38	Base composition (%) (T)	ECNC	0.004862588	291
## 39	Base composition (%) (G)	ECNC	-0.037787699	292
## 40	Base composition (%) (C)	ECNC	-0.037045693	293
## 41	Base composition (%) (Other)	ECNC	-0.040274294	294
## 42	# of sequences containing non-ACGTN (nt)	ECNC	-0.040587311	295
## 43	Mean sequence length (nt)	ECNC	-0.061569667	296
## 44	Median sequence length (nt)	ECNC	-0.060928944	297
## 45	Missing Proteins	ECNC	-0.062209031	298
## 46	#Prots	ECNC	-0.084046941	299
## 47	Completeness	ECNC	-0.084067608	300
## 48	Base composition (%) (N)	ECNC	0.013486259	301
## 49	totalLength	ECNC	0.061175951	302
## 50	Sum length of sequences > 1M (nt)	ECNC	0.046387082	303
## 51	# of sequences > 100K (nt)	ECNC	0.049326449	304
## 52	L50	ECNC	0.070430706	305
## 53	# of sequences > 1M (nt)	ECNC	0.063725329	306
## 54	# of sequences > 10M (nt)	ECNC	0.062895861	307
## 55	Shortest sequence (nt)	ECNC	-0.012113794	308
## 56	GC-content (%)	ECNC	-0.066249117	309
## 57	# of sequences	ECNC	0.070289641	310
## 58	# of sequences > 1K (nt)	ECNC	0.042151677	311
## 59	# of sequences > 10K (nt)	ECNC	0.041222984	312
## 60	#Total	ECNC	0.102797584	313
## 61	Average	ECNC	0.108543367	314
## 62	%Ortho	ECNC	0.104394790	315
## 63	Gene	CN	0.013089940	316
## 64	Genome	CN	-0.092501845	317

## 65	Sum length of sequences > 10M (nt)	CN	-0.061610123	318
## 66	Longest sequence (nt)	CN	-0.052591263	319
## 67	N50 sequence length (nt)	CN	-0.038770715	320
## 68	Base composition (%) (A)	CN	0.006139187	321
## 69	Base composition (%) (T)	CN	0.006354445	322
## 70	Base composition (%) (G)	CN	-0.036741673	323
## 71	Base composition (%) (C)	CN	-0.035971303	324
## 72	Base composition (%) (Other)	CN	-0.041544748	325
## 73	# of sequences containing non-ACGTN (nt)	CN	-0.041868348	326
## 74	Mean sequence length (nt)	CN	-0.063786387	327
## 75	Median sequence length (nt)	CN	-0.063541494	328
## 76	Missing Proteins	CN	-0.063703014	329
## 77	#Prots	CN	-0.085286259	330
## 78	Completeness	CN	-0.085306203	331
## 79	Base composition (%) (N)	CN	0.012122309	332
## 80	totalLength	CN	0.060342667	333
## 81	Sum length of sequences > 1M (nt)	CN	0.044889905	334
## 82	# of sequences > 100K (nt)	CN	0.047874628	335
## 83	L50	CN	0.069838784	336
## 84	# of sequences > 1M (nt)	CN	0.062839574	337
## 85	# of sequences > 10M (nt)	CN	0.062215472	338
## 86	Shortest sequence (nt)	CN	-0.013168670	339
## 87	GC-content (%)	CN	-0.066875760	340
## 88	# of sequences	CN	0.073563144	341
## 89	# of sequences > 1K (nt)	CN	0.044231140	342
## 90	# of sequences > 10K (nt)	CN	0.042436480	343
## 91	#Total	CN	0.105113732	344
## 92	Average	CN	0.110764419	345
## 93	%Ortho	CN	0.106456398	346

between genome quality scores-1.pdf

347



```
## Warning: Column 'Genome'/'BestGenome' joining factor and character vectors,
## coercing into character vector

## Warning: 'as.tibble()' is deprecated as of tibble 2.0.0.
## Please use 'as_tibble()' instead.
## The signature and semantics have changed, see '?as_tibble'.
## This warning is displayed once every 8 hours.
## Call 'lifecycle::last_warnings()' to see where this warning was generated.

## Warning: Removed 1 rows containing missing values (geom_text).

## Warning: Table 2
```

Enhanced cancer suppression may have evolved through many mechanisms; among the most parsimonious is an increase in the copy number of genes with tumor suppressor functions. Previous studies focusing on candidate gene studies, for example, have identified increased copy number of the tumor suppressors *TP53* and *LIF* in elephants [???,11,21–23]. Therefore, in order to test whether this was a pervasive phenomena genome-wide in *Afrotherians*, we used a Reciprocal Best Hit BLAT (RBHB) approach to infer gene copy number in *Afrotherian* and *Atlantogenatan* genomes (Fig. 2A). Because RBHB-like approaches can over-estimate copy number when genes are fragmented or incorrectly assembled across multiple scaffolds, we also inferred copy number using a complementary method that quantifies the ratio between observed and expected gene coverage per nucleotide (ECNC) (Fig. 2B; Sup. Fig. 2A-D). By only including nucleotides from the query sequence that were observed in the target genome,

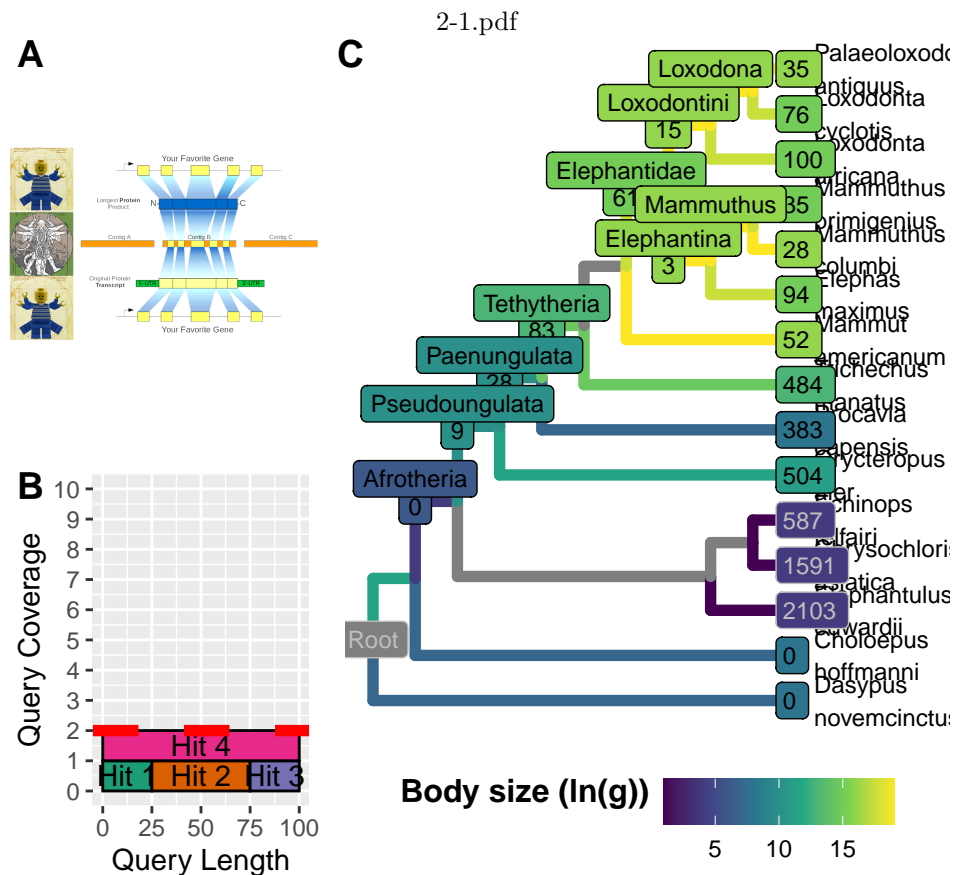


Fig 1. Figure 2: A Reciprocal Best-Hit BLAT pipeline for identifying gene copy number in other genomes. A) A graphic summary of the reciprocal best-hit strategy. B) Estimated Copy Number by Coverage. C)

we also correct for partial hits where some or all of the homologs of a gene have diverged from the human homolog.

Because our sequence database included various protein transcripts for each gene, in order to obtain gene-level copy number information and eliminate any many-to-one mappings of hits, we labeled each exon of every reciprocal best hit (RBH) with the gene corresponding to the query transcript and merged all overlapping exons; next, we eliminated any many-to-one exons that resulted from the previous step. Finally, we reassembled the gene loci based on the original transcript starts and ends, and the collapsed exon data, obtaining the full sequence of each RBH locus. Genes were considered to be duplicated if its copy number via RBHB was greater than or equal to 2, and the maximum ECNC among all transcripts prior to filtering was greater than or equal to 1.50. This cutoff of ECNC was selected to account for truncated gene duplications, which have been shown to be functional in various examples [???

examples of this]. To reconcile the Atlantogenatan phylogeny with duplication events, we used maximum likelihood to reconstruct likely ancestral copy numbers for each gene at each node in the phylogeny. To define the copy number of a gene, we conservatively used the lesser value between the RBHB hit count, and the ECNC value rounded to the nearest whole number. In order to perform

Next, in order to select genes and duplicates which were likely functional, we omitted any hits that were not supported by either the gene prediction method GenScan, or by at least one transcript assembled from publically-available RNA-seq data.

We describe the number of genes that increased in each lineage in *Atlantogenata* in Figure 2. Among the genes that increased in copy number in the elephant lineage are TP53 and LIF, as previously described. Furthermore, we identify

Duplications that occurred recently in Probodiscea are enriched for tumor suppressor pathways

In order to infer the functional consequences of these gene duplications, we tested if duplicate genes were enriched in specific pathways relative to our initial query set of genes. We used

Retroduplication of EEF1A1 in the stem-lineage of Tehthytheria

Warning: Fig 3: EEF1A1

Previous studies have identified genes whose transgenic overexpression delays aging related phenotypes and extends lifespan. Overexpression of the eukaryotic translation elongation factor 1 alpha 1 (EEF1A1) gene, for example, extends lifespan in transgenic *Drosophila*. Like most mammalian genomes, we found that Afrotherian genomes encoded numerous EEF1A1 retrogenes (Fig. XA). While the majority of these retrogenes have premature stop codons and insertions/deletions characteristic of pseudogenes, at least 13 Tehthytherian-specific EEF1A1 retrogenes have the potential to encode functional proteins (Fig. XB). Unfortunately it is difficult to determine if these retrogenes are transcribed because they have relatively high sequence similarity (83-88%), suggesting evidence of transcription using RNA-Seq data is likely an artifact. Indeed, nearly all of the EEF1A1 retrogene transcripts assembled by StringTie were confined to their gene body and UTRs and thus lacked unique sequences. The EEF1A1RTG13 transcript, however, initiates within an upstream MLT1B retrovirus-like MaLR transposable element and includes unique 5'- and 3'-UTR sequences, indicating at least one EEF1A1 retrogene is transcribed (Fig. XC). EEF1A1

Candidate gene studies, for example, have identified functional duplicates of the tumor suppressors TP53 and LIF in elephants. In a larger candidate gene study, Caulin et al. characterized the copy number of 830 known tumor-suppressor genes across 36 mammals and identified 382 putative duplicates, including duplicates in species with large body sizes and long life-spans. however, the probability of developing cancer is similar for small, short-lived mammals such as mice and for large, long-lived mammals such as elephants.

In stark contrast, genome-wide studies of unusually large or long-lived species such as the bowhead whale (Keane et al., 2015), Myotid bats (Seim et al., 2013; Zhang et al., 2013), naked mole rat (Kim et al., 2011), and blind mole rat (Fang et al., 2014) did not find an over representation of tumor suppressors among duplicate genes.

A genomic analysis of genetic changes associated with the evolution of enhanced cancer resistance in the elephant lineage has yet to be performed. Thus it is not clear if the duplication of TP53 and LIF reflects a general pattern of tumor suppressor duplication in the elephant lineage, unlike other lineages that resolved Peto's paradox, or from the kinds of ascertainment biases common in candidate gene studies.

Concerted duplication of TP53 and TP53-related genes towards *Probodiscea*

Warning: Fig4

Step-wise reduction of intrinsic cancer risk in large, long-lived Afrotherians

A tibble: 253 x 6

##	parent	node	branch.length	label	lnSize	Lifespan
##	<int>	<int>	<dbl>	<chr>	<dbl>	<dbl>
##	1	135	1	40.1	Geogale.aurita	2
##	2	140	2	122.	Limnogale.mergulus	5
##	3	140	3	0.135	Microgale.taiva	2
##	4	139	4	33.5	Microgale.parvula	1
##	5	138	5	0.595	Microgale.brevicaudata	2
##	6	142	6	0.571	Microgale.cowani	3
##	7	142	7	1.07	Microgale.jobihely	2
##	8	145	8	0.772	Microgale.longicaudata	2
##	9	145	9	0.173	Microgale.principula	2
##	10	144	10	34.3	Microgale.pusilla	1
##	11	143	11	61.4	Microgale.talazaci	4
##	12	136	12	22.8	Oryzorictes.hova	4
##	13	147	13	7.75	Echinops.telfairi	4
##	14	147	14	12.5	Setifer.setosus	6
##	15	148	15	4.68	Hemicentetes.semispinosus	5
##	16	148	16	79.5	Tenrec.ecaudatus	7
##	17	150	17	2.82	Micropotamogale.lamottei	4
##	18	150	18	103.	Potamogale.velox	6
##	19	151	19	69.8	Protenrec.tricuspis	1
##	20	151	20	2.21	Dilambdogale.gheerbranti	2
##	21	157	21	0.454	Carpitalpa.arendsi	4
##	22	158	22	3.26	Neamblysomus.gunningi	4
##	23	158	23	5.72	Neamblysomus.julianae	3
##	24	162	24	0.976	Amblysomus.corrae	4

##	25	162	25	1.38	Amblysomus.robustus	4	2.14
##	26	161	26	0.524	Amblysomus.septentrionalis	4	2.14
##	27	160	27	0.0152	Amblysomus.hottentotus	4	2.14
##	28	159	28	3.79	Amblysomus.marleyi	4	2.14
##	29	163	29	0.321	Chlorotalpa.duthieae	3	1.94
##	30	163	30	0.0874	Chlorotalpa.sclateri	4	2.14
##	31	165	31	62.8	Chrysospalax.trevelyani	6	2.50
##	32	165	32	0.130	Chrysospalax.villosus	5	2.30
##	33	164	33	13.4	Calcochloris.obtusirostris	3	1.94
##	34	153	34	9.65	Eremitalpa.granti	3	1.94
##	35	167	35	3.34	Chrysochloris.asiatica	4	2.14
##	36	167	36	5.78	Cryptochloris.wintoni	3	1.94
##	37	166	37	0.333	Chrysochloris.stuhlmanni	4	2.14
##	38	175	38	0.926	Elephantulus.brachyrhynchus	4	2.14
##	39	175	39	0.118	Elephantulus.rufescens	4	2.07
##	40	176	40	1.15	Elephantulus.intufi	4	2.23
##	41	176	41	0.319	Elephantulus.rupestris	4	2.14
##	42	177	42	0.237	Elephantulus.edwardii	4	2.14
##	43	177	43	0.953	Elephantulus.myurus	4	2.14
##	44	179	44	10.5	Elephantulus.rozeti	4	1.97
##	45	179	45	24.6	Petrodromus.tetradactylus	5	2.30
##	46	178	46	14.2	Macroscelides.probosceides	4	2.16
##	47	181	47	1.93	Elephantulus.fuscipes	4	2.14
##	48	182	48	0.678	Elephantulus.fuscus	4	2.14
##	49	182	49	1.10	Elephantulus.revoili	3	1.94
##	50	184	50	0.403	Rhynchocyon.chrysopygus	6	2.40
##	51	185	51	3.30	Rhynchocyon.cirnei	6	2.50
##	52	185	52	4.33	Rhynchocyon.udzungwensis	7	2.60
##	53	183	53	2.13	Rhynchocyon.petersi	6	2.50
##	54	170	54	15.9	Metoldobotes.sp..nov	6	2.50
##	55	186	55	11.8	Chambius.kasserinensis	4	2.14
##	56	186	56	11.6	Herodotius.pattersoni	5	2.30
##	57	188	57	6.59	Orycteropus.afer	11	3.39
##	58	188	58	0.569	Myorycteropus.africanus	10	3.27
##	59	194	59	1.86	Dendrohyrax.dorsalis	8	2.88
##	60	195	60	1.64	Heterohyrax.brucei	8	2.88
##	61	195	61	0.000068	Procavia.capensis	8	2.69
##	62	193	62	1.15	Thyrohyrax.domorictus	9	3.08
##	63	192	63	3.55	Thyrohyrax.meyeri	9	3.08
##	64	198	64	28.6	Thyrohyrax.litholagus	10	3.27
##	65	201	65	2.29	Pachyhyrax.crassidentatus	12	3.66
##	66	201	66	1.45	Bunohyrax.fajumensis	11	3.47
##	67	202	67	5.44	Geniohyus.mirus	11	3.47
##	68	202	68	11.4	Bunohyrax.major	12	3.66
##	69	203	69	0.235	Megalohyrax.eocaenus	12	3.66
##	70	203	70	7.21	Megalohyrax.sp..nov	13	3.86
##	71	207	71	0.0699	Titanohyrax.andrewsi	13	3.86
##	72	207	72	34.6	Titanohyrax.ultimus	14	4.05
##	73	206	73	0.0353	Titanohyrax.angustidens	12	3.66
##	74	205	74	13.7	Antilohyrax.pectidens	11	3.47
##	75	204	75	0.194	Afrohyrax.championi	11	3.47
##	76	209	76	2.90	Saghatherium.antiquum	10	3.27

##	77	209	77	15.0	Selenohyrax.chatrathi	11	3.47
##	78	208	78	15.8	Saghatherium.bowni	9	3.08
##	79	211	79	2.82	Seggeurius.amourensis	8	2.88
##	80	211	80	0.733	Microhyrax.lavocati	8	2.88
##	81	210	81	18.2	Dimaitherium.patnaiki	10	3.27
##	82	220	82	5.81	Elephas.maximus	15	4.18
##	83	222	83	6.12	Elephas.antiquus.falconeri	12	3.66
##	84	222	84	1.90	Elephas.cypriotes	12	3.66
##	85	221	85	0.340	Elephas.maximus.asurus	16	4.44
##	86	223	86	16.0	Mammuthus.trogontherii	16	4.44
##	87	224	87	0.910	Mammuthus.columbi	16	4.44
##	88	224	88	2.17	Mammuthus.primigenius	15	4.24
##	89	225	89	1.28	Loxodonta.africana	15	4.17
##	90	227	90	0.0149	Palaeoloxodon.antiquus	16	4.44
##	91	227	91	12.8	Palaeoloxodon.namadicus	17	4.63
##	92	226	92	3.72	Loxodonta.cyclotis	15	4.24
##	93	228	93	15.3	Mammut.borsoni	16	4.44
##	94	228	94	0.951	Mammut.americanum	16	4.44
##	95	216	95	3.64	Phiomia.spp	14	4.05
##	96	230	96	0.0280	Omanitherium.dhofarensis	13	3.86
##	97	230	97	7.29	Arcanotherium.savagei	13	3.86
##	98	229	98	73.6	Barytherium.spp	15	4.24
##	99	214	99	5.71	Moeritherium.spp	14	4.05
##	100	231	100	326.	Phosphatherium.escuilliei	10	3.27
##	101	232	101	2.29	Numidotherium.koholense	13	3.86
##	102	232	102	0.742	Daouitherium.rebouli	13	3.86
##	103	235	103	5.85	Dugong.dugon	13	4.29
##	104	235	104	173.	Hydrodamalis.gigas	16	4.44
##	105	237	105	0.688	Trichechus.inunguis	13	3.69
##	106	237	106	1.39	Trichechus.manatus	13	4.23
##	107	236	107	0.574	Trichechus.senegalensis	13	3.86
##	108	238	108	13.6	Prorastomus.sirenoides	11	3.47
##	109	238	109	33.7	Protosiren.smithae	13	3.86
##	110	241	110	0.640	Choloepus.didactylus	9	3.61
##	111	241	111	0.316	Choloepus.hoffmanni	8	3.71
##	112	242	112	0.0297	Bradypus.torquatus	8	2.88
##	113	243	113	0.483	Bradypus.tridactylus	8	2.88
##	114	243	114	0.512	Bradypus.variegatus	8	2.88
##	115	245	115	10.4	Tamandua.tetradactyla	9	2.94
##	116	245	116	41.0	Myrmecophaga.tridactyla	10	3.43
##	117	244	117	2.15	Cyclopes.didactylus	9	3.08
##	118	249	118	15.0	Euphractus.sexcinctus	8	3.10
##	119	249	119	5.54	Zaedyus.pichiy	7	2.53
##	120	250	120	0.0899	Chaetophractus.nationi	8	2.88
##	121	250	121	0.418	Chaetophractus.villosus	8	3.23
##	122	251	122	268.	Priodontes.maximus	11	2.71
##	123	252	123	16.0	Tolypeutes.matacus	7	3.61
##	124	252	124	0.248	Cabassous.centralis	8	2.88
##	125	253	125	4.05	Dasypus.hybridus	7	2.69
##	126	253	126	74.1	Dasypus.kappleri	9	3.08
##	127	253	127	14.7	Dasypus.novemcinctus	8	3.10
##	128	253	128	12.2	Dasypus.sabanicola	7	2.69

## 129	253	129	4.44	Dasypus.septemcinctus	7	2.82
## 130	130	130	NA	Atlantogenata	2	1.72
## 131	130	131	0.000982	Afrotheria	6	2.50
## 132	131	132	44.5	Afrosorcida	4	2.11
## 133	132	133	11.8	<NA>	4	2.11
## 134	133	134	0.420	<NA>	4	2.11
## 135	134	135	10.1	<NA>	3	1.91
## 136	135	136	0.373	<NA>	3	1.91
## 137	136	137	2.96	<NA>	3	1.91
## 138	137	138	2.69	<NA>	3	1.91
## 139	138	139	0.450	<NA>	2	1.72
## 140	139	140	3.36	<NA>	3	1.91
## 141	137	141	0.153	<NA>	3	1.91
## 142	141	142	0.116	<NA>	2	1.72
## 143	141	143	0.222	<NA>	2	1.72
## 144	143	144	0.771	<NA>	2	1.72
## 145	144	145	0.109	<NA>	3	1.91
## 146	134	146	38.5	<NA>	5	2.30
## 147	146	147	1.81	<NA>	3	1.91
## 148	146	148	5.26	<NA>	3	1.91
## 149	133	149	4.28	<NA>	3	1.91
## 150	149	150	52.3	<NA>	5	2.30
## 151	149	151	15.6	<NA>	3	1.91
## 152	132	152	12.0	<NA>	4	2.11
## 153	152	153	0.0295	<NA>	4	2.11
## 154	153	154	0.173	<NA>	3	1.91
## 155	154	155	0.0141	<NA>	3	1.91
## 156	155	156	0.107	<NA>	4	2.11
## 157	156	157	0.00544	<NA>	3	1.91
## 158	157	158	0.102	<NA>	3	1.91
## 159	156	159	0.150	<NA>	3	1.91
## 160	159	160	0.483	<NA>	3	1.91
## 161	160	161	0.321	<NA>	3	1.91
## 162	161	162	0.00743	<NA>	4	2.11
## 163	155	163	2.12	<NA>	3	1.91
## 164	154	164	0.774	<NA>	4	2.11
## 165	164	165	18.6	<NA>	5	2.30
## 166	152	166	0.260	<NA>	3	1.91
## 167	166	167	0.155	<NA>	3	1.91
## 168	131	168	0.00016	<NA>	6	2.50
## 169	168	169	2.49	Macroscelidae	5	2.30
## 170	169	170	0.105	<NA>	5	2.30
## 171	170	171	4.23	<NA>	5	2.30
## 172	171	172	6.20	<NA>	3	1.91
## 173	172	173	0.977	<NA>	3	1.91
## 174	173	174	0.448	<NA>	4	2.11
## 175	174	175	0.349	<NA>	4	2.11
## 176	174	176	0.176	<NA>	4	2.11
## 177	173	177	1.62	<NA>	4	2.11
## 178	172	178	0.155	<NA>	3	1.91
## 179	178	179	0.180	<NA>	4	2.11
## 180	171	180	0.100	<NA>	5	2.30

## 181	180	181	11.2	<NA>	3	1.91
## 182	181	182	12.0	<NA>	3	1.91
## 183	180	183	30.6	<NA>	3	1.91
## 184	183	184	2.34	<NA>	3	1.91
## 185	184	185	0.0165	<NA>	3	1.91
## 186	169	186	4.53	<NA>	5	2.30
## 187	168	187	546.	Pseudoungulata	10	3.27
## 188	187	188	12.9	<NA>	10	3.27
## 189	187	189	4.42	Paenungulata	10	3.27
## 190	189	190	6.90	<NA>	5	2.30
## 191	190	191	1.47	<NA>	10	3.27
## 192	191	192	17.9	<NA>	9	3.08
## 193	192	193	0.00758	<NA>	9	3.08
## 194	193	194	19.5	<NA>	5	2.30
## 195	194	195	2.67	<NA>	5	2.30
## 196	191	196	5.61	<NA>	3	1.91
## 197	196	197	8.46	<NA>	3	1.91
## 198	197	198	0.602	<NA>	11	3.47
## 199	198	199	8.81	<NA>	12	3.66
## 200	199	200	0.347	<NA>	3	1.91
## 201	200	201	0.177	<NA>	12	3.66
## 202	200	202	0.584	<NA>	3	1.91
## 203	199	203	8.90	<NA>	12	3.66
## 204	197	204	9.93	<NA>	11	3.47
## 205	204	205	1.23	<NA>	12	3.66
## 206	205	206	22.2	<NA>	3	1.91
## 207	206	207	10.2	<NA>	13	3.86
## 208	196	208	6.63	<NA>	3	1.91
## 209	208	209	1.16	<NA>	10	3.27
## 210	190	210	22.7	<NA>	9	3.08
## 211	210	211	8.32	<NA>	8	2.88
## 212	189	212	187.	Tethytheria	13	3.86
## 213	212	213	3.40	<NA>	3	1.91
## 214	213	214	6.37	<NA>	13	3.86
## 215	214	215	1.15	<NA>	14	4.05
## 216	215	216	13.4	<NA>	3	1.91
## 217	216	217	30.3	Proboscidae	3	1.91
## 218	217	218	2.21	Elephantidae	15	4.24
## 219	218	219	0.0116	Elephantina	16	4.44
## 220	219	220	0.128	<NA>	15	4.24
## 221	220	221	0.369	<NA>	3	1.91
## 222	221	222	400.	<NA>	3	1.91
## 223	219	223	0.645	<NA>	3	1.91
## 224	223	224	0.467	Mammuthus	16	4.44
## 225	218	225	0.108	Loxodontini	16	4.44
## 226	225	226	0.862	Loxodona	16	4.44
## 227	226	227	6.09	<NA>	3	1.91
## 228	217	228	9.63	<NA>	3	1.91
## 229	215	229	0.197	<NA>	3	1.91
## 230	229	230	2.47	<NA>	3	1.91
## 231	213	231	0.128	<NA>	13	3.86
## 232	231	232	0.268	<NA>	3	1.91

## 233	212	233	0.309	<NA>	12	3.66
## 234	233	234	16.4	<NA>	3	1.91
## 235	234	235	0.530	<NA>	3	1.91
## 236	234	236	0.134	<NA>	3	1.91
## 237	236	237	0.145	<NA>	3	1.91
## 238	233	238	3.59	<NA>	3	1.91
## 239	130	239	125.	Xenarthra	11	3.47
## 240	239	240	14.6	<NA>	3	1.91
## 241	240	241	3.04	<NA>	3	1.91
## 242	240	242	0.0660	<NA>	11	3.47
## 243	242	243	0.112	<NA>	11	3.47
## 244	239	244	15.1	<NA>	3	1.91
## 245	244	245	21.7	<NA>	9	3.08
## 246	239	246	0.958	<NA>	10	3.27
## 247	246	247	0.0602	<NA>	3	1.91
## 248	247	248	0.0914	<NA>	3	1.91
## 249	248	249	0.000579	<NA>	8	2.88
## 250	248	250	0.000908	<NA>	11	3.47
## 251	247	251	0.217	<NA>	3	1.91
## 252	251	252	0.0523	<NA>	11	3.47
## 253	246	253	0.140	<NA>	8	2.88

Warning: Fig5

The dramatic increase in body mass and lifespan in some Afrotherian lineages implies those lineages evolved reduced cancer risk. To infer the magnitude of these reductions we estimated differences in cancer risk between small bodied, short-lived species and large bodied, long-lived species as well as for reconstructed ancestral Afrotherians. Following [??] we estimate the intrinsic cancer risk as the product of risk associated with body mass and lifespan. Differences in cancer susceptibility due to body mass differences between species can be approximated simply as the fold difference in body mass (D) between species [??]. The risk of developing cancer also increases in proportion to the sixth power of age and is approximated by the formula Ct^6 , in which the proportionality constant C that determines susceptibility to cancer induction is multiplied by the sixth power of the age in years, t [??,??,??]. Thus we can estimate differences in the intrinsic cancer risk between species as $D(Ct^6)$. We inferred that susceptibility to cancer induction (C) was reduced 3.40×10^3 -fold in the ancestor of Pseudoungulata, 7.20×10^3 -fold in the ancestor of Paenungulata, 8.81×10^5 -fold in the ancestor of Tehthytheria, 1.46×10^8 -fold in the ancestor of Proboscidea, and 1.28×10^6 -fold in the ancestor of Sirenia relative to the ancestral Afrotherian (Table 3). What biological mechanisms underlie the evolution of thousand- to hundred million-fold reductions in cancer susceptibility during the origins of Afrotherians, which are essential for large body size and long lifespan to evolve

OTHER FIGURES

References

- Green J, Cairns BJ, Casabonne D, Wright FL, Reeves G, Beral V, et al. Height and cancer incidence in the Million Women Study: prospective cohort, and meta-analysis of prospective studies of height and total cancer risk. The Lancet Oncology. 2011;12:785–794. doi:10.1016/s1470-2045(11)70154-1

2. Nunney L. Size matters: height, cell number and a person's risk of cancer. *Proc R Soc B*. 2018;285: 20181743. doi:10.1098/rspb.2018.1743 720
3. Dobson JM. Breed-predispositions to cancer in pedigree dogs. *ISRN veterinary science*. 2013;2013: 941275. doi:10.1155/2013/941275 721
4. Caulin AF, Maley CC. Peto's Paradox: evolution's prescription for cancer prevention. *Trends in ecology & evolution*. 2011;26: 175–82. doi:10.1016/j.tree.2011.01.002 722
5. Leroi AM, Koufopanou V, Burt A. Cancer selection. *Nature Reviews Cancer*. 2003;3: 226–231. doi:10.1038/nrc1016 723
6. Peto R, Roe F, Lee P, Levy L, Clack J. Cancer and ageing in mice and men. *British Journal of Cancer*. 1975;32: 411–426. doi:10.1038/bjc.1975.242 724
7. Ashur-Fabian O, Avivi A, Trakhtenbrot L, Adamsky K, Cohen M, Kajakaro G, et al. Evolution of p53 in hypoxia-stressed *Spalax* mimics human tumor mutation. *Proceedings of the National Academy of Sciences*. 2004;101: 12236–12241. doi:10.1073/pnas.0404998101 725
8. Seluanov A, Hine C, Bozzella M, Hall A, Sasahara THC, Ribeiro AACM, et al. Distinct tumor suppressor mechanisms evolve in rodent species that differ in size and lifespan. *Aging cell*. 2008;7: 813–23. doi:10.1111/j.1474-9726.2008.00431.x 726
9. Gorbunova V, Hine C, Tian X, Abulaeva J, Gudkov AV, Nevo E, et al. Cancer resistance in the blind mole rat is mediated by concerted necrotic cell death mechanism. *Proceedings of the National Academy of Sciences of the United States of America*. 2012;109: 19392–6. doi:10.1073/pnas.1217211109 727
10. Tian X, Azpurua J, Hine C, Vaidya A, Myakishev-Rempel M, Abulaeva J, et al. High molecular weight hyaluronan mediates the cancer resistance of the naked mole-rat. 2013;499. doi:10.1038/nature12234 728
11. Sulak M, Fong L, Mika K, Chigurupati S, Yon L, Mongan NP, et al. TP53 copy number expansion is associated with the evolution of increased body size and an enhanced DNA damage response in elephants. *eLife*. 2016;5: e11994. doi:10.7554/elife.11994 729
12. Tacutu R, Craig T, Budovsky A, Wuttke D, Lehmann G, Taranukha D, et al. Human Ageing Genomic Resources: Integrated databases and tools for the biology and genetics of ageing. *Nucleic Acids Research*. 2013;41: D1027–D1033. doi:10.1093/nar/gks1155 730
13. Schwartz GT, Rasmussen DT, Smith RJ. Body-Size Diversity and Community Structure of Fossil Hyracoids. *Journal of Mammalogy*. 1995;76: 1088–1099. doi:10.2307/1382601 731
14. Scheffer VB. The Weight of the Steller Sea Cow. *Journal of Mammalogy*. 1972;53: 912–914. doi:10.2307/1379236 732
15. Larramendi A. Shoulder Height, Body Mass, and Shape of Proboscideans. *Acta Palaeontologica Polonica*. 2015;61. doi:10.4202/app.00136.2014 733
16. O'Leary MA, Bloch JI, Flynn JJ, Gaudin TJ, Giallombardo A, Giannini NP, et al. The placental mammal ancestor and the post-K-Pg radiation of placentals. *Science* (New York, NY). 2013;339: 662–7. doi:10.1126/science.1229237 734
17. Springer MS, Meredith RW, Teeling EC, Murphy WJ. Technical comment on "The placental mammal ancestor and the post-K-Pg radiation of placentals". *Science* (New York, NY). 2013;341: 613. doi:10.1126/science.1238025 735
18. O'Leary MA, Bloch JI, Flynn JJ, Gaudin TJ, Giallombardo A, Giannini NP, et al. Response to comment on "The placental mammal ancestor and the post-K-Pg radiation of placentals". *Science* (New York, NY). 2013;341: 613. doi:10.1126/science.1238162 736
19. Puttick MN, Thomas GH. Fossils and living taxa agree on patterns of body mass evolution: a case study with Afrotheria. *Proceedings Biological sciences / The Royal* 737

Society. 2015;282: 20152023. doi:10.1098/rspb.2015.2023 772

20. Abegglen LM, Caulin AF, Chan A, Lee K, Robinson R, Campbell MS, et al. 773
 Potential Mechanisms for Cancer Resistance in Elephants and Comparative Cellular 774
 Response to DNA Damage in Humans. JAMA. 2015;314: 1850–1860. 775
 doi:10.1001/jama.2015.13134 776

21. Vazquez JM, Sulak M, Chigurupati S, Lynch VJ. A Zombie LIF Gene in 777
 Elephants Is Upregulated by TP53 to Induce Apoptosis in Response to DNA Damage. 778
 Cell Reports. 2018;24: 1765–1776. doi:10.1016/j.celrep.2018.07.042 779

22. Caulin AF, Graham TA, Wang L-S, Maley CC. Solutions to Peto’s paradox 780
 revealed by mathematical modelling and cross-species cancer gene analysis. 781
 Philosophical transactions of the Royal Society of London Series B, Biological sciences. 782
 2015;370: 20140222. doi:10.1098/rstb.2014.0222 783

23. Doherty A, Magalhães J de. Has gene duplication impacted the evolution of 784
 Eutherian longevity? Aging Cell. 2016;15: 978–980. doi:10.1111/ace.12503 785

24. Bininda-Emonds ORP, Cardillo M, Jones KE, MacPhee RDE, Beck RMD, 786
 Grenyer R, et al. Erratum: The delayed rise of present-day mammals. Nature. 787
 2008;456: 274–274. doi:10.1038/nature07347 788

25. Elliot MG, Mooers AØ. Inferring ancestral states without assuming neutrality or 789
 gradualism using a stable model of continuous character evolution. BMC evolutionary 790
 biology. 2014;14: 226. doi:10.1186/s12862-014-0226-8 791

26. Kent JW. BLAT—The BLAST-Like Alignment Tool. Genome Research. 792
 2002;12: 656–664. doi:10.1101/gr.229202 793

27. Altenhoff AM, Dessimoz C. Phylogenetic and functional assessment of orthologs 794
 inference projects and methods. PLoS computational biology. 2009;5: e1000262. 795
 doi:10.1371/journal.pcbi.1000262 796

28. Consortium TU. UniProt: the universal protein knowledgebase. Nucleic Acids 797
 Research. 2017;45: D158–D169. doi:10.1093/nar/gkw1099 798